# A larger brown fat volume and lower radiodensity are related to a greater cardiometabolic risk, especially in young men

Acosta, F.M.; Sanchez-Delgado, G.; Martinez-Tellez, B.; Osuna-Prieto, F.J.; Mendez-Gutierrez, A.; Aguilera, C.M.; ... ; Ruiz, J.R.

# A larger brown fat volume and lower radiodensity are related to a greater cardiometabolic risk, especially in young men

**Francisco M Acosta**[1,2,3,4], **Guillermo Sanchez-Delgado**[1,5], **Borja Martinez-Tellez**[1,6], **Francisco J Osuna-Prieto**[1,7,8], **Andrea Mendez-Gutierrez**[9,10,11], **Concepcion M Aguilera**[9,10,11], **Angel Gil**[9,10,11], **Jose M Llamas-Elvira**[12] and **Jonatan R Ruiz**[1,10]

[1]PROFITH 'PRO-moting FITness and Health Through Physical Activity' Research Group, Department of Physical and Sports Education, Sport and Health University Research Institute (iMUDS), Faculty of Sports Science, University of Granada, Granada, Spain, [2]Turku PET Centre, University of Turku, Turku, Finland, [3]Turku PET Centre, Turku University Hospital, Turku, Finland, [4]InFLAMES Research Flagship Center, University of Turku, Turku, Finland, [5]Pennington Biomedical Research Center, Baton Rouge, Louisiana, USA, [6]Division of Endocrinology, and Einthoven Laboratory for Experimental Vascular Medicine, Department of Medicine, Leiden University Medical Center, Leiden, The Netherlands, [7]Department of Analytical Chemistry, University of Granada, Granada, Spain, [8]Research and Development of Functional Food Center (CIDAF), Granada, Spain, [9]Department of Biochemistry and Molecular Biology II, 'José Mataix Verdú' Institute of Nutrition and Food Technology (INYTA), Biomedical Research Centre (CIBM), University of Granada, Granada, Spain, [10]Instituto de Investigación Biosanitaria, ibs.Granada, Granada, Spain, [11]CIBER Fisiopatología de la Obesidad y la Nutrición (CIBEROBNISCIII), Madrid, Spain, and [12]Nuclear Medicine Services, 'Virgen de las Nieves' University Hospital, Granada, Spain

Correspondence should be addressed to F M Acosta or J R Ruiz
**Email** fm.acostamanzano@gmail.com or ruizj@ugr.es

## Abstract

*Objectives:* Brown adipose tissue (BAT) is important in the maintenance of cardiometabolic health in rodents. Recent reports appear to suggest the same in humans, although if this is true remains elusive partly because of the methodological bias that affected previous research. This cross-sectional work reports the relationships of cold-induced BAT volume, activity (peak standardized uptake, $SUV_{peak}$), and mean radiodensity (an inverse proxy of the triacylglycerols content) with the cardiometabolic and inflammatory profile of 131 young adults, and how these relationships are influenced by sex and body weight.

*Design:* This is a cross-sectional study.

*Methods:* Subjects underwent personalized cold exposure for 2 h to activate BAT, followed by static $^{18}$F-fluorodeoxyglucose PET-CT scanning to determine BAT variables. Information on cardiometabolic risk (CMR) and inflammatory markers was gathered, and a CMR score and fatty liver index (FLI) were calculated.

*Results:* In men, BAT volume was positively related to homocysteine and liver damage markers concentrations (independently of BMI and seasonality) and the FLI (all $P \leq 0.05$). In men, BAT mean radiodensity was negatively related to the glucose and insulin concentrations, alanine aminotransferase activity, insulin resistance, total cholesterol/HDL-C, LDL-C/HDL-C, the CMR score, and the FLI (all $P \leq 0.02$). In women, it was only negatively related to the FLI ($P < 0.001$). These associations were driven by the results for the overweight and obese subjects. No relationship was seen between BAT and inflammatory markers ($P > 0.05$).

*Conclusions:* A larger BAT volume and a lower BAT mean radiodensity are related to a higher CMR, especially in young men, which may support that BAT acts as a compensatory organ in states of metabolic disruption.

*European Journal of Endocrinology* (2022) **187**, 171–183

https://eje.bioscientifica.com
https://doi.org/10.1530/EJE-22-0130



Published by Bioscientifica Ltd.

## Introduction

In 2009, it was confirmed that brown adipose tissue (BAT), a thermogenic organ with great potential to prevent obesity and cardiometabolic disease in rodents, was metabolically active in adult humans (1). Since then, BAT has been shown to dissipate energy as heat mainly via the catabolism of glucose and fatty acids (2, 3). Further, BAT can potentially modulate metabolism body-wide via the secretion of immunometabolic factors (4). Although the likelihood of human BAT having a role as an anti-obesity agent is low given its scant contribution to daily energy expenditure (10–13 kcal/day when cold-stimulated) (5), it is still to be determined whether it may be beneficial in terms of cardiometabolic risk (CMR) management.

Studies in rodents support the latter idea (2, 6, 7). However, in humans, the evidence is inconclusive, in part because of the difficulty in designing appropriate experiments, the existence of important confounders, and the lack of mechanistic insight in most earlier work (8, 9, 10, 11, 12, 13). Recently, a retrospective study analysed BAT volume and activity via $^{18}$F-fluorodeoxyglucose PET-CT ($^{18}$F-FDG-PET-CT) in 52 487 patients with cancer (8), and the results suggested it to be associated with improved cardiometabolic health, especially in patients with overweight or obesity. However, as in other previous studies, the $^{18}$F-FDG-PET-CT scanning was performed at thermoneutrality, a condition under which functional BAT is likely undetectable. Indeed, to avoid this bias, current recommendations state that $^{18}$F-FDG–PET-CT scanning should be performed after individualized cold exposure (14). A clear need exists for data to be collected in new experiments that take all these issues into account.

The present cross-sectional study explores the relationship shown by the cold-induced BAT volume and activity (estimated by $^{18}$F-FDG-PET-CT) and BAT mean radiodensity (an indicator of biological tissue density which is inversely related to triacylglycerols content) (15) with the cardiometabolic and inflammatory profile in a large cohort of relatively healthy, young adults. Special attention was paid to the influence of sex and body weight on these relationships (factors that in previous studies were mostly overlooked), and analyses performed that took into account potential confounders. In addition, BARCIST recommendations were strictly adhered to when analysing all $^{18}$F-FDG-PET-CT-related variables.

## Subjects and methods

### Study subjects and experimental design

This study was performed as part of the ACTIBATE project (ClinicalTrials.gov no. NCT02365129) (16). Subjects were recruited via advertisements in electronic media and leaflets. The inclusion criteria were to be 18–25 years old, to be sedentary (self-reported <20 min moderate-vigorous physical activity on <3 days/week), to be a non-smoker, to have had a steady body weight over the last 3 months (change <3 kg), to have no cardiometabolic disease (hypertension, diabetes, etc.), not to be pregnant, and not to be regularly exposed to cold environments (e.g. as would be ski monitors or fishmongers). Written, signed, informed consent to be included was obtained from all subjects. All study protocols adhered to the 2013 Declaration of Helsinki and were approved by the Human Research Ethics Committee of the University of Granada (no. 924), and by the Human Research Ethics Committee of the *Junta de Andalucía* (no. 0838-N-2017). All assessments were made in Granada (Spain).

### Procedures

All subjects underwent $^{18}$F-FDG-PET-CT scanning (to assess BAT variables) over eight dates distributed between October and December 2015 and 2016, that is four dates per year, with one test per subject. The cardiometabolic and inflammatory profiles, anthropometry, body composition, and lifestyle behaviours were recorded within 3 weeks of the $^{18}$F-FDG-PET-CT assessment.

### $^{18}$F-FDG-PET-CT scanning

Subjects came to the participating hospital and asked to confirm that they had met the pre-study conditions, i.e.: (i) to be arriving in a fasting state (and have been so for at least 6 h); (ii) having slept as usual; (iii) having refrained from any moderate or vigorous physical activity (within 24 and 48 h respectively); (iv) having not consumed any alcohol or stimulant (e.g. caffeine) beverages in the previous 6 h. Subjects were then asked to void their bladder and to dress in standardized clothes (sandals, shorts, and T-shirt) and were directed to a quiet, warm (22–23°C) room where they were seated for 30 min. After this period, the subjects were

moved into an air-conditioned cold room (19.5–20°C) where they sat down and were put on a temperature-controlled water-perfused cooling vest (Polar Products Inc., Stow, OH, USA), which covered the clavicular region, the chest, the abdomen, and the back. The water temperature of the cooling vest was set 4°C above their individual shivering threshold, which was determined 48–72 h before $^{18}$F-FDG-PET-CT scanning (17). Subjects remained under these conditions for 60 min to induce BAT activation. They were then injected with a bolus of $^{18}$F-FDG (183.52 ± 12.21 MBq), with the water temperature of the cooling vest raised by ~1°C for the last 60 min to avoid shivering (or whenever subjects reported shivering). After 2 h, all subjects lay supine in a whole-body PET-CT scanner, and a low-dose CT scan (120 kV) was performed for attenuation correction and anatomic localization, followed by static PET consisting of two-bed position scans from the atlas vertebra to the mid-chest (6 min each).

The date when the baseline PET-CT scan was performed was recorded as the day of the year (January 1 = day 1, and December 31 = day 365/366; a means of recording the season of the year).

## $^{18}$F-FDG-PET-CT analysis

PET-CT scans were semi-automatically analysed using the Beth Israel plug-in for FIJI http://sourceforge.net/projects/bifijiplugins/. To determine BAT volume and peak standardized uptake value ($SUV_{peak}$), six regions of interest (ROIs) were outlined from the atlas vertebra to thoracic vertebra 4 using a 3D-axial technique. These ROIs comprised the supraclavicular, laterocervical, paravertebral, and mediastinal regions. To determine BAT mean radiodensity, an ROI covering the scanned body – except the mouth – was outlined from the atlas vertebra to the thoracic vertebra 4. Within these ROIs, the SUV threshold for a voxel to be considered to represent BAT was taken as ≥(1.2/(lean body mass/body mass)); the radiodensity also had to fall in the range −190 to −10 Hounsfield units (HU) (14, 18). The mean BAT volume (average of all ROIs) and $SUV_{peak}$ (i.e. the highest average SUV in a 1-mL spherical volume overall ROIs), and the BAT mean radiodensity were recorded (see Supplementary Fig. 1 (see section on supplementary materials given at the end of this article) for a visual description of BAT variables). Subjects were classified as PET+ when they had a BAT volume higher than 7.78 mL (these subjects had a substantial number of BAT voxels within the outlined ROIs) or as PET− if their BAT volume was lower than 7.78 mL. This was determined visually for each PET-CT image. It should be noted that since a whole ROI was drawn to determine BAT mean radiodensity, which included areas where BAT is not typically located, some voxels belonging to connective tissue, internal organs, glands, etc., were erroneously classified as BAT in the PET− subjects ($n$ = 31); these subjects were not included in BAT mean radiodensity determinations. A single-slice ROI was also outlined to determine the $SUV_{peak}$ in the subcutaneous white adipose tissue (used as a reference tissue) next to the triceps brachialis. For the sake of confirmation, BAT $SUV_{peak}$ was recalculated as a product of the percentage lean body mass ($SUV_{LBM}$).

## Cardiometabolic and inflammatory profiles

On a different day, subjects came for the collection of blood samples, at which time they were asked to confirm they met the same requirements as outlined above (see $^{18}$F-FDG-PET-CT scanning). Samples were collected in BD Vacutainer® collection tubes, centrifuged, and the serum collected sent to analyse the glycaemic, lipid, hepatic, and several inflammatory markers (C-reactive protein, C3, C4, and β-microglobulin 2) concentrations (see below). Plasma samples were aliquoted in smaller volumes and frozen at −80°C for the later analysis of other inflammatory markers (see below).

### *Glycaemic, lipid and other markers, and the HOMA index*

Serum glucose, total cholesterol, (HDL-C), triacylglycerol, and homocysteine concentrations were measured following standard colorimetric methods using an AU5832 automated analyser (Beckman Coulter Inc., Brea, CA, USA). Serum insulin was measured using the Access Ultrasensitive Insulin Chemiluminescent Immunoassay Kit (Beckman Coulter Inc.). LDL-C was estimated as (total cholesterol − HDL-C − (triacylglycerols/5)), in mg/dL (19), and other cardiovascular risk indices, including the total cholesterol/HDL-C and LDL-C/HDL-C ratios, were calculated. Insulin resistance was determined via the homeostatic model assessment of insulin resistance (HOMA-IR) using the equation (insulin (μU/mL) × glucose (mmol/L))/22.5, and via the homeostatic model assessment of beta-cell function (HOMA-β) using the equation (20 × insulin (μU/mL))/((glucose (mmol/L) − 3.5) (20, 21).

### *Systolic, diastolic, and mean blood pressure*

Systolic and diastolic blood pressure was measured with the subjects seated and relaxed, using an Omron M6 upper arm blood pressure monitor (Omron Healthcare Europe B.V.

Hoofddorp, The Netherlands). Measurements were taken on three different days, and the mean was determined for use in later analyses. Mean blood pressure was calculated as: (systolic blood pressure + (2 × diastolic blood pressure))/3.

### *Cardiometabolic risk score*

A CMR score based on variables included in the diagnostic criteria of metabolic syndrome (22) was calculated using a model that includes subject waist circumference, mean blood pressure, glucose, and HDL-C and triacylglycerol concentrations. Each variable was standardized as follows: standardized value = (value − mean)/S.D. The HDL-C standardized values were multiplied by −1 in keeping with the negative scores for the other CMRs. The final score was determined as the average of the five standardized scores. The final CMR score was calculated separately for men and women.

### *Hepatic enzymes and fatty liver index*

The serum alanine aminotransferase, gamma-glutamyl transferase (GGT), and alkaline phosphatase (ALP) activities were determined by standard colorimetric methods, using an AU5832 automated analyser (Beckman Coulter Inc.). The fatty liver index (FLI) was calculated as a simple but accurate predictor of hepatic steatosis in the general population (23). A FLI of <30 was used to rule out hepatic steatosis, whereas a value of >60 was used to indicate its presence (23).

### *Inflammatory markers*

Serum C-reactive protein, C3, C4, and β-microglobulin 2 concentrations were measured by immunoturbidimetric assay, employing the same AU5832 automated analyser as above. Plasma interleukin (IL)-2, IL-4, IL-6, IL-7, IL-8, IL-10, IL-17a, interferon-gamma (IFNγ), and tumor necrosis factor-alpha (TNFα) were determined using the MILLIPLEX MAP Human High Sensitivity Cytokine Panel (Luminex Corp., Clayton, MO, USA). Leptin and adiponectin concentrations were measured using Panels 1 and 2 (respectively) of the MILLIPLEX MAG/MAP Human Adipokine Magnetic Bead Kits (Luminex Corp.).

## Anthropometry, body composition, and lifestyle behaviours

Anthropometry (weight, height, BMI, and waist circumference), body composition (including fat and lean mass, and visceral adipose tissue (VAT) mass), and lifestyle behaviours (including sedentary behaviour, physical activity, sleep duration, energy and macronutrient intake, and habitual dietary patterns) were determined as reported elsewhere (17, 24, 25) and detailed in Supplementary Appendix A.

## Statistical analysis

Continuous variables are presented as means (S.D.) when normally distributed or medians (interquartile range) when not. Categorical variables are presented as numbers (percentage). The effect of the interaction between BAT variables and sex on the cardiometabolic and inflammatory profiles was examined by linear regression. Since an interaction effect was observed for several outcomes, all analyses were performed separately for men and women. Several extreme cases, confirmed as influential outliers with respect to the outcome variables, were corrected using a subtle version of winsorizing (Supplementary Appendix B). In some cases, optimum Box-Cox transformations were employed to normalize the data.

Potential confounders (i.e. according to prior evidence (24, 25, 26, 27, 28)) or that were statistically related to predictors/outcomes were included in the models used in the primary and sensitivity analyses. Multiple linear regression was used to analyse the relationship shown by BAT volume, $SUV_{peak}$, and mean radiodensity with the cardiometabolic and the inflammatory profiles (Tables 1 and 2, respectively). Adjustments were then made for BMI and for BMI plus the PET-CT scan date. The associations between BAT variables and the FLI were not adjusted for BMI in any model since this was one of the components included in the algorithm to calculate the FLI. Additional analyses were performed to determine whether the relationships shown by the BAT variables with the cardiometabolic and inflammatory profiles were dependent on body weight. Body weight was classified as normal weight (BMI ≥18 and <25 kg/m$^2$), overweight (BMI ≥25 and <30 kg/m$^2$), or obese (BMI ≥30 kg/m$^2$) in analyses related to BAT volume and $SUV_{peak}$, and as normal weight and overweight-obese in analyses related to BAT mean radiodensity (a reduced number of obese subjects were available for this analysis). Adjustments for multiple comparison errors (familywise error rate (Hochberg procedure)) were made for the main analyses (Tables 1 and 2).

Analyses were performed using SPSS-26.0 software (IBM). Significance was set at $P \leq 0.05$ for the linear correlation and regression analyses and at $P < 0.1$ for the effects of interactions.

**Table 1** Associations shown by BAT volume, $SUV_{peak}$, and mean radiodensity with cardiometabolic risk (CMR) markers in young men and women. Linear regression analyses were performed. The non-standardized regression coefficient (B), S.E., standardized regression coefficient (β), and adjusted R squared (Adj. $R^2$) are provided. A subtle variation of winsorizing was performed on the extreme outliers of outcome results, and some variables were transformed using Box-Cox transformations (see Supplementary Appendix B). Transformed variables are unitless. Similar results were observed with outliers corrected and not corrected, except for the association of BAT $SUV_{peak}$ with the homocysteine concentration, and of BAT mean radiodensity with HOMA-B (which were non-significant; $P > 0.05$), and of BAT $SUV_{peak}$ with ALT levels (which were significant; $P < 0.05$) when outliers were corrected for the men.

| | BAT volume | | | | | BAT $SUV_{peak}$ | | | | | BAT mean radiodensity | | | | |
|---|---|---|---|---|---|---|---|---|---|---|---|---|---|---|---|
| | B | S.E. | β | Adj. $R^2$ | *P* | B | S.E. | β | Adj. $R^2$ | *P* | B | S.E. | β | Adj. $R^2$ | *P* |
| Men (*n* = 45)* | | | | | | | | | | | | | | | |
| Glucose (mg/dL) | 0.009 | 0.017 | 0.081 | −0.016 | 0.59 | 0.079 | 0.151 | 0.079 | −0.017 | 0.60 | −0.345 | 0.139 | −0.418 | 0.146 | **0.02** |
| Insulin (uIU/mL) | 0.017 | 0.013 | 0.194 | 0.015 | 0.20 | 0.055 | 0.119 | 0.071 | −0.018 | 0.64 | −0.409 | 0.101 | −0.600 | 0.337 | **<0.001** |
| HOMA-IR | 0.004 | 0.003 | 0.177 | 0.009 | 0.24 | 0.011 | 0.030 | 0.058 | −0.020 | 0.71 | −0.107 | 0.025 | −0.622 | 0.366 | **<0.001** |
| HOMA-β | 0.218 | 0.134 | 0.240 | 0.036 | 0.11 | 0.600 | 1.254 | 0.073 | −0.018 | 0.63 | −3.499 | 1.191 | −0.479 | 0.097 | **0.006** |
| Total cholesterol (mg/dL) | 0.118 | 0.068 | 0.254 | 0.043 | 0.09 | 0.485 | 0.639 | 0.115 | −0.010 | 0.45 | −0.296 | 0.666 | −0.082 | −0.027 | 0.66 |
| LDL-C (mg/dL) | 0.086 | 0.055 | 0.232 | 0.032 | 0.12 | 0.301 | 0.512 | 0.089 | −0.015 | 0.56 | −0.621 | 0.544 | −0.207 | −0.01 | 0.26 |
| HDL-C (mg/dL) | 0.028 | 0.017 | 0.247 | 0.039 | 0.10 | 0.193 | 0.153 | 0.189 | 0.013 | 0.21 | 0.394 | 0.133 | 0.482 | 0.206 | **0.006** |
| Total cholesterol/HDL-C | 0.001 | 0.002 | 0.083 | −0.016 | 0.59 | −0.002 | 0.018 | −0.018 | −0.023 | 0.91 | −0.039 | 0.016 | −0.410 | −0.140 | **0.022** |
| LDL-C/HDL-C | 0.001 | 0.002 | 0.066 | −0.019 | 0.66 | −0.004 | 0.015 | −0.040 | −0.022 | 0.79 | −0.034 | 0.013 | −0.435 | 0.161 | **0.015** |
| Triacylglycerols | 0.002 | 0.003 | 0.143 | −0.002 | 0.35 | 0.021 | 0.024 | 0.132 | −0.005 | 0.39 | −0.010 | 0.026 | −0.068 | −0.030 | 0.72 |
| Homocysteine (μmol/L) | 0.018 | 0.007 | 0.383 | 0.127 | **0.009** | 0.109 | 0.062 | 0.258 | 0.045 | 0.09 | 0.049 | 0.062 | 0.145 | −0.013 | 0.44 |
| Systolic BP (mmHg) | 0.022 | 0.025 | 0.139 | −0.004 | 0.37 | 0.181 | 0.224 | 0.124 | −0.008 | 0.42 | −0.343 | 0.236 | −0.265 | 0.037 | 0.16 |
| Diastolic BP[a] (mmHg) | 0.018 | 0.020 | 0.137 | −0.004 | 0.37 | −0.047 | 0.182 | −0.040 | −0.022 | 0.80 | −0.270 | 0.167 | −0.293 | −0.053 | 0.12 |
| **CMR score** | 0.002 | 0.002 | 0.171 | 0.006 | 0.27 | 0.009 | 0.020 | 0.070 | −0.019 | 0.65 | −0.064 | 0.016 | −0.596 | 0.332 | **0.001** |
| ALT[a] | 0.004 | 0.002 | 0.270 | 0.051 | 0.07 | 0.020 | 0.022 | 0.142 | −0.003 | 0.35 | −0.059 | 0.023 | −0.425 | 0.153 | **0.02** |
| GGT[a] | 0.005 | 0.002 | 0.381 | 0.125 | **0.01** | 0.029 | 0.017 | 0.249 | 0.040 | 0.10 | −0.029 | 0.020 | −0.257 | 0.034 | 0.16 |
| ALP (U/L) | 0.088 | 0.036 | 0.346 | 0.099 | **0.02** | 0.591 | 0.340 | 0.256 | 0.044 | 0.09 | −0.128 | 0.376 | −0.063 | −0.030 | 0.74 |
| **FLI** | 0.005 | 0.002 | 0.348 | 0.101 | **0.02** | 0.018 | 0.018 | 0.152 | 0 | 0.32 | −0.069 | 0.016 | −0.618 | 0.360 | **<0.001** |
| Women (*n* = 86)† | | | | | | | | | | | | | | | |
| Glucose (mg/dL) | 0.014 | 0.012 | 0.123 | 0.003 | 0.20 | 0.031 | 0.074 | 0.045 | −0.010 | 0.68 | 0.035 | 0.074 | 0.059 | −0.012 | 0.64 |
| Insulin (uIU/mL) | 0.004 | 0.008 | 0.058 | −0.009 | 0.60 | 0.023 | 0.051 | 0.048 | −0.010 | 0.66 | −0.065 | 0.045 | −0.178 | 0.016 | 0.15 |
| HOMA-IR | 0.001 | 0.002 | 0.061 | −0.008 | 0.57 | 0.005 | 0.013 | 0.043 | −0.010 | 0.69 | −0.015 | 0.011 | −0.159 | 0.010 | 0.20 |
| HOMA-β | 0.018 | 0.095 | 0.021 | −0.011 | 0.85 | 0.294 | 0.578 | 0.055 | −0.009 | 0.61 | −0.922 | 0.502 | −0.224 | 0.035 | 0.07 |
| Total cholesterol (mg/dL) | −0.09 | 0.091 | −0.159 | 0.014 | 0.14 | -0.543 | 0.371 | −0.158 | 0.013 | 0.15 | 0.403 | 0.359 | 0.139 | 0.004 | 0.27 |
| LDL-C (mg/dL) | −0.07 | 0.049 | −0.153 | 0.012 | 0.16 | −0.387 | 0.303 | −0.138 | 0.007 | 0.20 | 0.244 | 0.265 | 0.114 | −0.002 | 0.36 |
| HDL-C (mg/dL) | −0.009 | 0.021 | −0.047 | −0.010 | 0.67 | −0.056 | 0.129 | −0.047 | −0.010 | 0.66 | 0.210 | 0.124 | 0.207 | 0.028 | 0.10 |
| Total cholesterol/HDL-C | −0.002 | 0.001 | −0.148 | 0.010 | 0.17 | −0.009 | 0.007 | −0.132 | 0.006 | 0.22 | −0.005 | 0.006 | −0.107 | −0.004 | 0.39 |
| LDL-C/HDL-C | −0.001 | 0.001 | −0.136 | 0.007 | 0.21 | −0.007 | 0.007 | −0.116 | 0.002 | 0.29 | −0.003 | 0.006 | −0.073 | −0.010 | 0.56 |
| Triacylglycerols | −0.002 | 0.002 | −0.149 | 0.010 | 0.17 | −0.012 | 0.011 | −0.120 | 0.003 | 0.27 | −0.005 | 0.011 | −0.059 | −0.471 | 0.64 |
| Homocysteine (μmol/L) | −0.005 | 0.005 | −0.102 | −0.001 | 0.35 | −0.013 | 0.031 | −0.045 | −0.010 | 0.68 | 0.041 | 0.030 | 0.166 | 0.012 | 0.18 |
| Systolic BP (mmHg) | −0.002 | 0.190 | −0.012 | −0.012 | 0.92 | 0.051 | 0.117 | 0.048 | −0.010 | 0.66 | 0.041 | 0.112 | 0.047 | −0.014 | 0.71 |
| Diastolic BP[a] (mmHg) | 0.002 | 0.013 | 0.015 | −0.012 | 0.89 | 0.026 | 0.080 | 0.036 | −0.011 | 0.74 | −0.009 | 0.068 | −0.017 | −0.016 | 0.89 |
| **CMR score** | 0.001 | 0.002 | 0.065 | −0.008 | 0.56 | 0 | 0.013 | −0.004 | −0.012 | 0.97 | −0.012 | 0.010 | −0.151 | 0.007 | 0.24 |
| ALT[a] | 0 | 0.002 | 0.005 | -0.012 | 0.96 | 0.001 | 0.010 | 0.011 | 0.012 | 0.92 | −0.002 | 0.009 | −0.025 | −0.015 | 0.84 |
| GGT[a] | −0.001 | 0.002 | −0.080 | −0.005 | 0.46 | −0.016 | 0.010 | −0.169 | 0.017 | 0.12 | −0.004 | 0.009 | −0.054 | −0.013 | 0.67 |
| ALP (U/L) | 0.022 | 0.036 | −0.068 | −0.007 | 0.53 | −0.403 | 0.213 | -0.202 | 0.029 | 0.06 | −0.445 | 0.207 | −0.260 | 0.053 | **0.03** |
| **FLI** | 0 | 0.002 | 0.010 | −0.012 | 0.93 | −0.017 | 0.011 | −0.162 | 0.014 | 0.14 | −0.022 | 0.009 | −0.296 | 0.073 | **0.02** |

Outcomes with the superscript [a] had one missing subject; **n* = 31 for BAT mean radiodensity; †*n* = 66 for BAT mean radiodensity. Significant relationships ($P \leq 0.05$) are shown in bold.
ALP, alkaline phosphatase; ALT, alanine aminotransferase; BAT, brown adipose tissue; GGT, gamma-glutamyl transferase; HOMA-IR, homeostatic model assessment of insulin resistance; HOMA-β, homeostatic model of β-cell function; SUV, standardized uptake value.

**Table 2** Associations shown by BAT volume, $SUV_{peak}$, and mean radiodensity with inflammatory markers in young men and women. The non-standardized regression coefficient (B), S.E., standardized regression coefficient (β), adjusted $R^2$ (Adj. $R^2$) and P values are provided. A subtle variation of winsorizing was performed on the extreme outliers of outcome results, and some variables were transformed using Box-Cox transformations (see Supplementary Appendix B). Transformed variables are unitless. Similar results were observed with outliers corrected and uncorrected, except for the association of BAT volume with adiponectin levels – which was significant ($P < 0.05$) – and of BAT mean radiodensity with IL-10 levels (which was non-significant; $P > 0.05$) when outliers were not corrected in women.

| | BAT volume | | | | | BAT $SUV_{peak}$ | | | | | BAT mean radiodensity | | | | |
|---|---|---|---|---|---|---|---|---|---|---|---|---|---|---|---|
| | B | S.E. | β | Adj. $R^2$ | *P* | B | S.E. | β | Adj. $R^2$ | *P* | B | S.E. | β | Adj. $R^2$ | *P* |
| Men, *n* = 45* | | | | | | | | | | | | | | | |
| C-reactive protein | 0.003 | 0.002 | 0.216 | 0.024 | 0.15 | 0.025 | 0.018 | 0.203 | 0.019 | 0.18 | −0.029 | 0.019 | −0.280 | 0.046 | 0.13 |
| IL-2[a] (pg/mL) | −0.004 | 0.004 | −0.201 | 0.015 | 0.22 | −0.053 | 0.029 | −0.284 | 0.056 | 0.08 | −0.027 | 0.030 | −0.184 | −0.008 | 0.38 |
| IL-4[a] | −0.002 | 0.003 | −0.126 | −0.011 | 0.44 | −0.019 | 0.023 | −0.136 | -0.008 | 0.41 | −0.031 | 0.026 | −0.238 | 0.016 | 0.25 |
| IL-6[a] (pg/mL) | −0.003 | 0.005 | −0.091 | −0.018 | 0.58 | −0.019 | 0.038 | −0.080 | −0.020 | 0.63 | −0.035 | 0.040 | −0.177 | −0.011 | 0.40 |
| IL-7[a] | −0.001 | 0.003 | −0.034 | −0.026 | 0.83 | −0.010 | 0.022 | −0.075 | −0.021 | 0.65 | −0.026 | 0.023 | −0.228 | 0.011 | 0.27 |
| IL-8[a] | −0.003 | 0.003 | −0.183 | 0.007 | 0.27 | −0.029 | 0.024 | −0.198 | 0.013 | 0.23 | −0.033 | 0.026 | −0.260 | 0.027 | 0.21 |
| IL-10[a] (pg/mL) | −0.006 | 0.006 | −0.166 | 0.001 | 0.31 | −0.041 | 0.048 | −0.139 | −0.007 | 0.40 | 0.001 | 0.053 | 0.003 | −0.043 | 0.99 |
| IL-17a[a] (pg/mL) | −0.005 | 0.005 | −0.153 | −0.003 | 0.35 | −0.087 | 0.044 | −0.307 | 0.070 | 0.06 | −0.039 | 0.055 | −0.146 | −0.021 | 0.49 |
| IFNγ[a] (pg/mL) | −0.016 | 0.013 | −0.187 | 0.009 | 0.25 | −0.118 | 0.113 | −0.170 | 0.003 | 0.30 | 0.031 | 0.120 | 0.054 | −0.040 | 0.80 |
| TNFα[a] (pg/mL) | −0.003 | 0.002 | −0.226 | 0.026 | 0.17 | −0.016 | 0.015 | −0.167 | 0.002 | 0.31 | 0.006 | 0.014 | 0.085 | −0.036 | 0.69 |
| Complement 3 (mg/dL) | 0.167 | 0.053 | 0.434 | 0.170 | **0.003** | 1.159 | 0.506 | 0.330 | 0.088 | **0.03** | −1.145 | 0.509 | −0.385 | 0.119 | **0.03** |
| Complement 4 (mg/dL) | 0.021 | 0.022 | 0.146 | −0.001 | 0.34 | 0.258 | 0.197 | 0.195 | 0.016 | 0.20 | 0.029 | 0.208 | 0.026 | −0.034 | 0.89 |
| B2-microglobulin (mg/L) | 0 | 0 | 0.041 | −0.022 | 0.79 | 0.003 | 0.004 | 0.106 | −0.012 | 0.49 | 0.006 | 0.005 | 0.243 | 0.026 | 0.19 |
| Adiponectin[b] (mg/L) | 0.005 | 0.012 | 0.068 | −0.019 | 0.66 | 0.096 | 0.111 | 0.132 | −0.006 | 0.39 | 0.285 | 0.108 | 0.445 | 0.169 | **0.01** |
| Leptin[c] (μg/L) | 0.006 | 0.011 | 0.101 | −0.018 | 0.55 | 0.094 | 0.098 | 0.160 | −0.002 | 0.34 | −0.019 | 0.112 | −0.036 | −0.042 | 0.87 |
| Women, *n* = 86[†] | | | | | | | | | | | | | | | |
| C-reactive protein | 0.005 | 0.002 | 0.230 | 0.041 | **0.03** | 0.016 | 0.013 | 0.135 | 0.006 | 0.22 | −0.024 | 0.012 | −0.237 | 0.041 | **0.05** |
| IL-2[a] (pg/mL) | 0.002 | 0.003 | 0.082 | −0.008 | 0.50 | 0.020 | 0.018 | 0.137 | 0.004 | 0.26 | 0.017 | 0.019 | 0.121 | −0.004 | 0.38 |
| IL-4[a] | 0.002 | 0.002 | 0.093 | −0.005 | 0.43 | 0.012 | 0.013 | 0.117 | −0.001 | 0.34 | 0.009 | 0.013 | 0.092 | −0.011 | 0.51 |
| IL-6[a] (pg/mL) | 0.001 | 0.004 | 0.024 | −0.014 | 0.84 | 0.013 | 0.022 | 0.068 | −0.010 | 0.58 | −0.012 | 0.024 | −0.069 | −0.014 | 0.62 |
| IL-7[a] | 0.001 | 0.002 | 0.080 | −0.008 | 0.51 | 0.024 | 0.012 | 0.225 | 0.037 | 0.06 | 0.022 | 0.013 | 0.225 | 0.032 | 0.10 |
| IL-8[a] | 0 | 0.002 | 0.010 | −0.015 | 0.94 | 0.008 | 0.013 | 0.077 | −0.009 | 0.53 | 0.002 | 0.014 | 0.020 | −0.019 | 0.88 |
| IL-10[a] (pg/mL) | 0.004 | 0.006 | 0.082 | −0.008 | 0.50 | 0.046 | 0.035 | 0.156 | 0.010 | 0.20 | 0.096 | 0.037 | 0.334 | 0.095 | **0.01** |
| IL-17a[a] (pg/mL) | 0.001 | 0.004 | 0.018 | −0.014 | 0.88 | 0.008 | 0.027 | 0.037 | −0.013 | 0.76 | 0.025 | 0.030 | 0.117 | −0.005 | 0.40 |
| IFNγ[a] (pg/mL) | 0.007 | 0.011 | 0.078 | −0.009 | 0.52 | 0.033 | 0.071 | 0.056 | −0.011 | 0.64 | 0.105 | 0.077 | 0.185 | 0.016 | 0.18 |
| TNFα[a] (pg/mL) | −0.001 | 0.002 | −0.092 | −0.006 | 0.45 | −0.006 | 0.011 | −0.061 | −0.011 | 0.62 | 0.008 | 0.011 | 0.099 | −0.009 | 0.48 |
| Complement 3 (mg/dL) | 0.043 | 0.043 | 0.109 | 0 | 0.32 | −0.062 | 0.266 | −0.025 | −0.011 | 0.82 | −0.519 | 0.255 | −0.246 | 0.046 | **0.05** |
| Complement 4 (mg/dL) | 0.023 | 0.016 | 0.154 | 0.012 | 0.16 | 0.090 | 0.099 | 0.098 | −0.002 | 0.37 | −0.077 | 0.098 | −0.098 | −0.006 | 0.43 |
| B2-microglobulin (mg/L) | 0 | 0 | 0.090 | −0.004 | 0.41 | −0.001 | 0.003 | −0.043 | −0.010 | 0.69 | 0.002 | 0.003 | 0.087 | −0.008 | 0.49 |
| Adiponectin[b] (mg/L) | 0.023 | 0.015 | 0.170 | 0.017 | 0.13 | 0.070 | 0.090 | 0.086 | −0.005 | 0.44 | 0.113 | 0.086 | 0.165 | 0.011 | 0.20 |
| Leptin[c] (μg/L) | 0 | 0.008 | 0.002 | −0.013 | 0.98 | −0.037 | 0.048 | −0.088 | −0.005 | 0.44 | 0.043 | 0.053 | 0.106 | −0.006 | 0.42 |

Some specific outcomes had missing data for men: [a]6 missing subjects, [b]1 missing subjects, [c]8 missing subjects; and for women: [a]16 missing subjects, [b]4 missing subjects, [c]7 missing subjects. **n* = 31 for BAT mean radiodensity; [†]*n* = 66 for BAT mean radiodensity. Significant relationships ($P \leq 0.05$) are shown in bold.

BAT, brown adipose tissue; IFNγ, interferon-gamma; IL, interleukin; SUV, standardized uptake value; TNFα, tumor necrosis factor-alpha.

## Results

A total of 131 subjects (86 women) were included in this study (see flow chart, Supplementary Fig. 2). Supplementary Table 1 shows the main characteristics of the study subjects.

### A larger BAT volume and lower BAT mean radiodensity are related to increased cardiometabolic risk, especially in young men

In men, but not women, BAT volume was positively associated with the homocysteine, GGT and ALP activities, and the FLI (all $P \leq 0.02$, Table 1). In men, BAT mean radiodensity was positively related to the HDL-C concentrations and inversely related to the glucose and insulin concentrations, HOMA-IR, HOMA-B, TC/HDL-C and LDL-C/HDL-C, to the CMR score, and the FLI (all $P \leq 0.02$).

In women, BAT mean radiodensity was negatively related to the ALP activity and the FLI (all $P \leq 0.03$). Figure 1 shows the scatter plots for the associations between the BAT variables and the CMR score and FLI, both in terms of subject sex and body weight.

When all these analyses were repeated adjusting for BMI, or for the BMI and PET-CT scan date (data not shown), the association between BAT volume and the HDL-C concentration became significant ($P = 0.01$), and the associations between BAT mean radiodensity and the CMR markers became non-significant (all $P > 0.05$) – except for the HDL-C concentration in men. After adjusting for multiplicity, all associations were non-significant in women (all $P > 0.05$), as were the associations between BAT mean radiodensity and most of the CMR markers in men, although its associations with the insulin levels, HOMA-IR, CMR score, and the FLI remained significant (all $P \leq 0.01$).

### BAT variables are not related to inflammatory markers

In men, BAT volume and $SUV_{peak}$ were positively related to the C3 concentration; BAT mean radiodensity was negatively related to the C3 concentration and positively to the adiponectin concentrations (all $P \leq 0.03$, Table 2). In women, BAT volume was positively associated with the C-reactive protein concentration, whereas BAT mean radiodensity was negatively related to it and the C3 concentration, but positively related to the IL-10 concentration. When these analyses were adjusted for BMI, or for BMI and the PET-CT scan date, the associations between BAT mean radiodensity and adiponectin (in men) and C3 (in women) became non-significant ($P > 0.05$, data not shown). After adjusting for multiplicity, all associations became non-significant ($P > 0.05$).

### Body weight influenced the relationship shown by BAT variables with cardiometabolic risk and inflammatory markers

The relationship shown by the BAT variables with the CMR and inflammatory markers were also examined in men and women according to their body weight (see Fig. 2); BMI has previously been reported to influence these variables (27) (see Supplementary Table 2).

In men, BAT volume was positively related to the total cholesterol, LDL-C, and homocysteine concentrations in the overweight group ($r = 0.56$–$0.65$, all $P < 0.06$), and to the HDL-C ($r = 0.7$, $P = 0.008$) in the obesity group. Further, in men with obesity, BAT mean radiodensity was inversely related to the glucose and insulin concentrations, and the HOMA-IR and HOMA-B scores ($r = -0.61$ to $-0.75$, all $P < 0.09$), and positively related to HDL-C ($r = 0.54$, $P \leq 0.09$). However, none of these associations was observed in women (all $P > 0.05$). Similarly, heterogeneous patterns were observed for the associations between BAT variables and inflammatory markers. Supplementary Figures 3 and 4 show the scatter plots for all the significant relationships detected. It should be noted that the PET-CT scan date was similar across all groups (all $P > 0.05$, see Supplementary Fig. 5).

Sensitivity analyses important for the interpretation of the current results are provided in the Supplementary Appendix C.

## Discussion

This study examines the relationships shown by BAT volume, $SUV_{peak}$, and mean radiodensity with the CMR and inflammatory markers for the largest cohort of young adults in which BAT $^{18}$F-FDG uptake has been assessed following individualized cold exposure, and strictly adhering to current methodological recommendations. The young age of the subjects likely prevents the $^{18}$F-FDG results from being biased by age-induced BAT dysfunction. In contrast to that reported in previous studies, the present findings suggest that a higher BAT volume and a lower BAT mean radiodensity are associated with increased CMR, especially in young men. Body weight greatly influenced all the associations shown by BAT volume

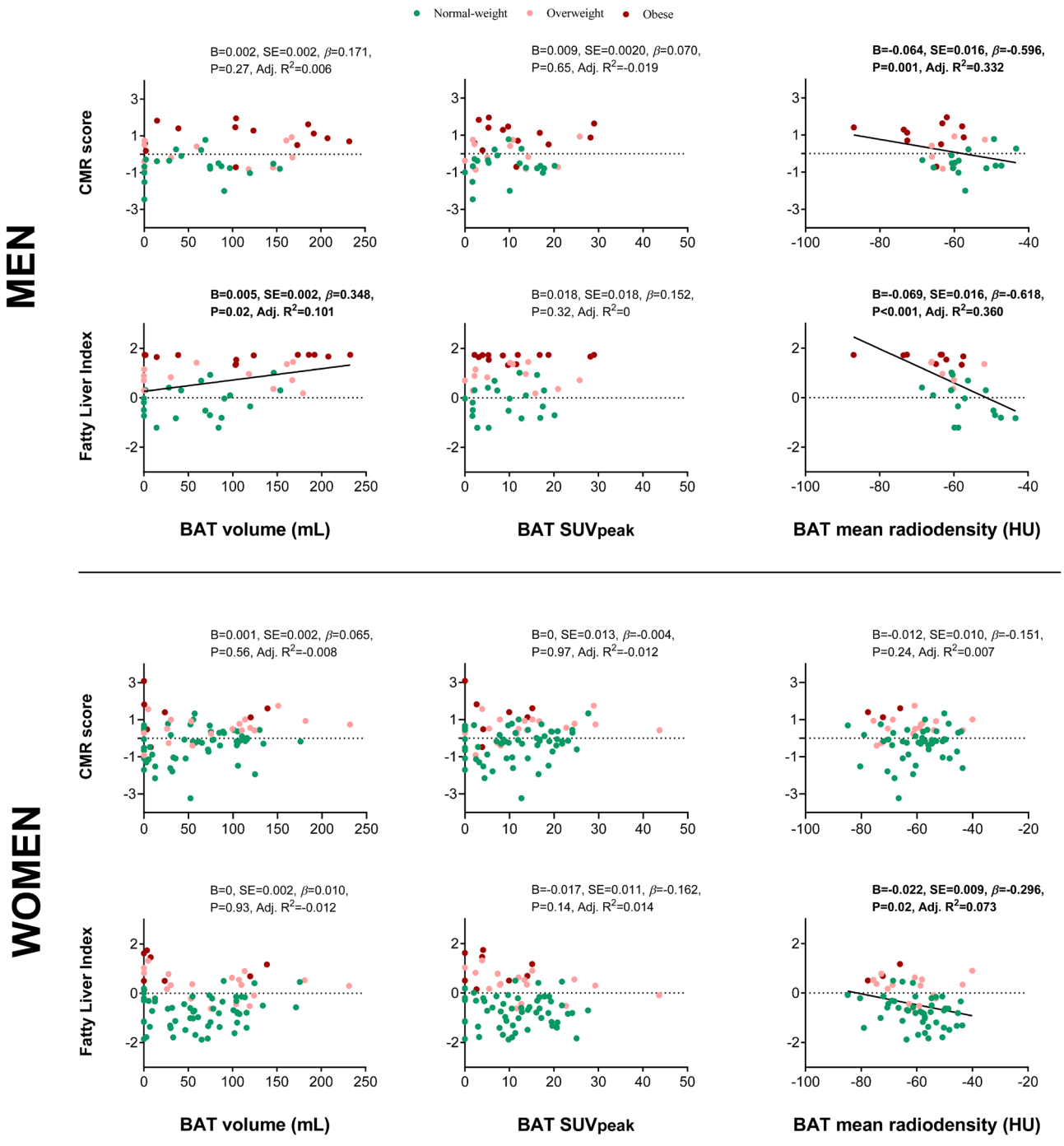


**Figure 1**

Scatter plots for linear regressions involving BAT volume, $SUV_{peak}$, or mean radiodensity against the cardiometabolic risk (CMR) score and the fatty liver index, in young men and women (Table 2). B: non-standardized regression coefficient, S.E., β: standardized regression coefficient, and Adj. $R^2$: adjusted R squared are provided. The CMR score and fatty liver index were winsorized and transformed. The sample size for men was 45 (except for BAT mean radiodensity, $n$ = 31) and for women 86 (except for BAT mean radiodensity, $n$ = 66). BAT, brown adipose tissue; CMR, cardiometabolic risk; SUV, standardized uptake value. A full colour version of this figure is available at https://doi.org/10.1530/EJE-22-0130.

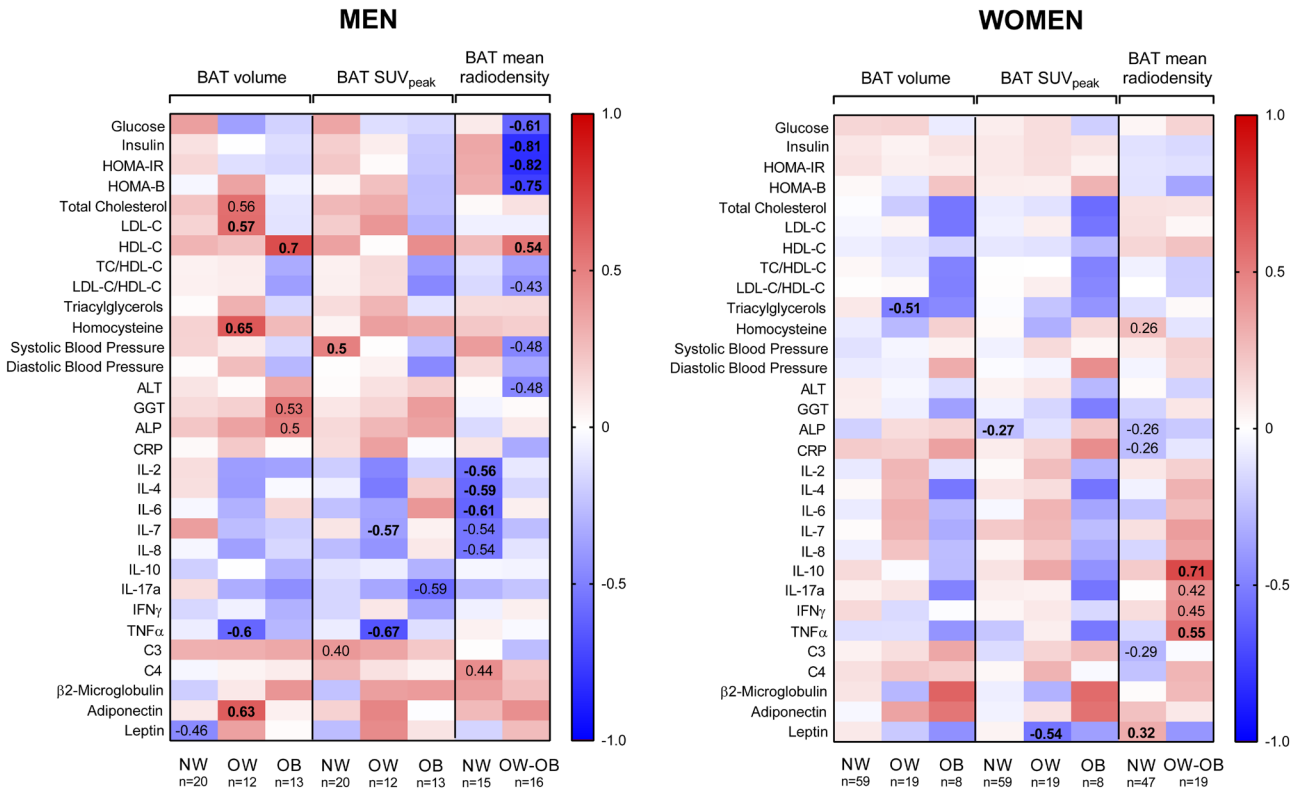


**Figure 2**

Associations shown by BAT volume, $SUV_{peak}$, and mean radiodensity with cardiometabolic risk and inflammatory markers in young men and women, according to the subject body weight. The heat map shows the strength of the Pearson correlations; the darker the colour of the square, the stronger the correlation is (the dark red colour represents a Pearson coefficient of 1, and the dark blue colour represents a negative Pearson coefficient of −1). The Pearson correlation coefficient is provided for those associations with a *P* value of ≤0.1 and is shown in bold for significant associations of $P \leq 0.05$. A subtle variation of winsorizing was performed on the extreme outliers of outcome results, and some variables were transformed using Box–Cox transformations (Supplementary Appendix B). Some specific outcomes had some missing data for men: 1 missing subject for systolic and diastolic blood pressure, adiponectin, 6 for IL-2, IL-4, IL-6, IL-7, IL-8, IL-10, IL-17a, IFN, TNFα, and 8 for leptin; and for women: 1 missing for systolic and diastolic blood pressure, ALT, GGT, 3 for FLI, 4 for adiponectin, 7 for leptin, and 16 for IL-2, IL-4, IL-6, IL-7, IL-8, IL-10, IL-17a, IFN, and TNFα. ALP, alkaline phosphatase; ALT, alanine aminotransferase; BAT, brown adipose tissue; GGT, gamma-glutamyl transferase; HOMA-IR, homeostatic model assessment of insulin resistance; HOMA-β, homeostatic model of β-cell function; IFNγ, interferon-gamma; IL, interleukin; SUV, standardized uptake value; TC, total cholesterol; TNFα, tumor necrosis factor-alpha. A full colour version of this figure is available at https://doi.org/10.1530/EJE-22-0130.

and mean radiodensity with the CMR markers – being these associations driven by the results for the overweight and obese subjects. BAT variables were not related to inflammatory marker concentrations. These findings call into question the results reported in previous retrospective studies performed at thermoneutrality and provide new insight into the role of BAT in cardiometabolic health.

Recent studies in adult humans have suggested that a larger BAT volume/prevalence (assessed by static $^{18}$F-FDG-PET-CT) or a lower supraclavicular fat fraction (assessed by MRI), either in warm (8, 13) or cold conditions (10, 29), are related to better cardiometabolic health. In contrast, the present results suggest that a larger BAT volume is related to an increase in several markers of CMR, especially in men. The lack of prior evidence regarding how BAT volume relates to CMR in men and women precludes any comparison. However, it is well known that men preferentially accumulate fat in the upper body adipose depots (e.g. VAT), whereas premenopausal women accumulate fat mainly in the gluteofemoral depots; this prompts the regularly observed higher CMR in men (30). It might therefore be speculated that in men with elevated

CMR markers, BAT could be recruited to help maintain metabolic homeostasis. This hypothesis is in line with the classic studies of Rothwell and Stock (31), showing that obesity induced in mice by cafeteria or high-fat diets is accompanied by an increase in BAT mass. Accordingly, men with a higher overall and central adiposity have a larger cold-activated BAT volume (27), and young men with obesity have a larger BAT volume compared to their normal-weight peers (in the present work, 85% were PET+, see Supplementary Fig. 6). Another possibility to consider is that in states of metabolic disruption, such as obesity, excess energy could lead to increased lipid storage and expansion of BAT (as well as of other tissues) – although this would be probably accompanied by a decreased BAT metabolic activity, and this does not appear to be the case in the current study.

The discrepancies between the present and previous studies (10, 11, 12, 13) cannot be explained by a single factor. For example, in a cohort like ours, the young age of our subjects and the low prevalence of insulin resistance – both factors related to impaired BAT $^{18}$F-FDG uptake (32) – are less likely to bias the $^{18}$F-FDG related measures than when examining older or diseased populations. In addition, most previous studies have involved a small sample size, preventing confounders (e.g. environmental temperature, age, lifestyle behaviours), or the influence of sex being taken into account. In addition, the methodological approach has varied greatly across studies. For instance, few studies exposed subjects to cooling before performing a BAT $^{18}$F-FDG-PET-CT scan, an oversight likely to render a large proportion of the functional BAT undetectable, biasing the results. Moreover, many studies did not follow the international BARCIST recommendations for measuring and analysing BAT $^{18}$F-FDG variables (14).

Should future studies show that BAT recruitment is important for metabolic homeostasis in humans, the underlying mechanisms will need to be investigated. It has been argued that BAT may contribute directly to the prevention of obesity and the reduction of CMR by increasing daily energy expenditure and systemic glucose and non-esterified fatty acid (NEFA) turnover – although so far the indications are that this is unlikely (3, 5, 33). However, rodent experiments show that BAT may also act through indirect mechanisms or via the release of different immunometabolic factors, modulating whole-body metabolism (4, 6, 7). For instance, when exposed to cold, murine BAT generates small HDL particles, accelerating HDL turnover and reducing cholesterol transport to the liver (34). Paradoxically, in the present work, subjects with a larger BAT volume had higher levels of HDL-C (when adjusted for BMI or BMI plus the PET-CT scan date), even though BAT volume was positively related to CMR markers. Future studies are needed to ascertain the significance of this finding, but it may support an indirect role for BAT in the regulation of human metabolism (conserved even in states of metabolic disruption). Certainly, it has been shown that brown fat-secreted factor neuregulin 4 preserves metabolic homeostasis via the attenuation of hepatic lipogenesis (35), and positive associations between BAT volume with activities of hepatic enzymes, and with the FLI (a proxy of hepatic steatosis (23)), are shown in the present work. This may support the importance of a BAT–liver axis for maintaining metabolic homeostasis.

The present findings also show that men with a higher CMR had a lower BAT mean radiodensity. Indeed, systemic markers/scores of insulin resistance, insulin secretion dysfunction, dyslipidemia, and hepatic dysfunction were related to lower BAT mean radiodensity in men, and those men with metabolic syndrome had a lower BAT mean radiodensity (Supplementary Fig. 7). Accordingly, we recently reported that overall and central adiposity were moderately related to lower BAT mean radiodensity in men, and weakly related to this in women (27). It is known that in obesity, lipids tend to accumulate in ectopic depots, promoting lipotoxic effects such as insulin resistance or inflammation, which lead to tissue dysfunction (36) – and this may also be the case with human BAT. Indeed, BAT glucose and NEFA uptake and perfusion are reduced in subjects with obesity compared to their lean counterparts in warm and cold conditions (15, 37). In addition, the correlation between BAT mean radiodensity and the FLI may indicate that ectopic lipid accumulation in both tissues occurs (in parallel) in obesity or states of metabolic disruption.

A recent study (8) reported that PET+ subjects (i.e. with detectable BAT) had better cardiometabolic health than those who were PET−, with more pronounced effects in patients with overweight or obesity. It is noteworthy, however, that $^{18}$F-FDG PET-CT scans were performed in warm conditions, and most subjects were qualitatively classified as having BAT or not. In addition, that work contained many old and/or diseased persons, some of whom were insulin resistant (i.e. had impaired BAT $^{18}$F-FDG uptake (32)), which limited the conclusions that could be drawn on the moderating role of body weight on the relationships observed. The present work, however, reveals that associations shown by BAT volume and BAT

mean radiodensity with CMR markers occur in men with overweight/obesity. This suggests that the contribution of the BAT to metabolic regulation might be more significant in states of metabolic disruption, such as obesity.

## Limitations of the study

The present results should be interpreted with caution; the cross-sectional study design precludes the establishment of causal relationships. Further, the sample was composed of young, relatively healthy men and women; this could have masked or weakened the associations of the BAT variables with the CMR and inflammatory profiles. Although the use of the shivering threshold as the end point of the personalized cold exposure is widely used in the field, it could have affected the thermal stress to which each subject was submitted, introducing differences in BAT variables results (38). BAT $^{18}$F-FDG uptake was quantified using the most commonly employed technique and following current recommendations (14). However, static $^{18}$F-FDG-PET-CT scans suffer several limitations that may prevent a fully accurate estimation of cold-induced BAT metabolic activity (39). Finally, the multiplicity and sensitivity analyses should be considered when interpreting the present results.

In conclusion, the present results suggest that a larger BAT volume and a lower BAT mean radiodensity are associated with an increased CMR, especially in young men. Body weight greatly influences the associations between BAT variables and CMR – associations observed only in the overweight and obese groups. BAT variables were not related to inflammatory markers. Future studies should investigate whether these findings are replicated in other populations, and in longitudinal studies, and determine the underlying mechanisms linking BAT and cardiometabolic health.

**Supplementary materials**

This is linked to the online version of the paper at https://doi.org/10.1530/EJE-22-0130.

**Declaration of interest**

The authors declare that there is no conflict of interest that could be perceived as prejudicing the impartiality of the research reported.

**Funding**

This study was funded by the Spanish Ministry of Economy and Competitiveness via the *Fondo de Investigación Sanitaria del Instituto de Salud Carlos III* (PI13/01393) and PTA 12264-I, by *Retos de la Sociedad* (DEP2016-79512-R), European Regional Development Funds (ERDF), the Spanish Ministry of Education (FPU 13/03410, FPU16/02828, FPU16/03653), the *Fundación Iberoamericana de Nutrición* (FINUT), the *Redes Temáticas de Investigación Cooperativa* RETIC network (Red SAMID RD16/0022), the AstraZeneca HealthCare Foundation, the University of Granada's *Plan Propio de Investigación 2016* – Excellence actions: Unit of Excellence on Exercise and Health (UCEES), the *Junta de Andalucía, Consejería de Conocimiento, Investigación y Universidades* (ERDF, SOMM17/6107/UGR), and *Consejería de Economía, Conocimiento, Empresas y Universidad* (P18-624 RT-4455), the *Fundación Alfonso Martin Escudero*, and the *InFLAMES Flagship Programme* of the Academy of Finland (decision no.: 337530).

**Author contribution statement**

F A M, G S D, B M T, C M A, A G, J M L L E, and J R R designed the study; F A M, G S D, B M T, and A M G conducted the experiments; C M A, A G, J M L L E, and J R R provided essential reagents and materials; F A M, G S D, B M T, F J O P, and A M G analysed the data and performed the statistical analysis; F A M wrote the manuscript; F A M, G S D, B M T, F J O P, A M G, C M A, A G, J M L L E, and J R R reviewed the manuscript and provided scientific assistance; F A M and J R R are the guarantors of this work and, as such, had full access to all the data in the study and take responsibility for the integrity of the data and the accuracy of the data analysis.

## References

1 Virtanen KA, Lidell ME, Orava J, Heglind M, Westergren R, Niemi T, Taittonen M, Laine J, Savisto NJ, Enerbäck S *et al.* Functional brown adipose tissue in healthy adults. *New England Journal of Medicine* 2009 **360** 1518–1525. (https://doi.org/10.1056/NEJMoa0808949)

2 Ruiz JR, Martinez-Tellez B, Sanchez-Delgado G, Osuna-Prieto FJ, Rensen PCN & Boon MR. Role of human brown fat in obesity, metabolism and cardiovascular disease: strategies to turn up the heat. *Progress in Cardiovascular Diseases* 2018 **61** 232–245. (https://doi.org/10.1016/j.pcad.2018.07.002)

3 Carpentier AC, Blondin DP, Virtanen KA, Richard D, Haman F & Turcotte ÉE. Brown adipose tissue energy metabolism in humans. *Frontiers in Endocrinology* 2018 **9** 447. (https://doi.org/10.3389/fendo.2018.00447)

4 Villarroya F, Cereijo R, Villarroya J & Giralt M. Brown adipose tissue as a secretory organ. *Nature Reviews: Endocrinology* 2017 **13** 26–35. (https://doi.org/10.1038/nrendo.2016.136)

5 Din UM, Raiko J, Saari T, Kudomi N, Tolvanen T, Oikonen V, Teuho J, Sipilä HT, Savisto N, Parkkola R *et al.* Human brown adipose tissue [15O]O2 PET imaging in the presence and absence of cold stimulus. *European Journal of Nuclear Medicine and Molecular Imaging* 2016 **43** 1878–1886. (https://doi.org/10.1007/s00259-016-3364-y)

6 Stanford KI, Middelbeek RJW, Townsend KL, An D, Nygaard EB, Hitchcox KM, Markan KR, Nakano K, Hirshman MF, Tseng YH *et al.* Brown adipose tissue regulates glucose homeostasis and insulin sensitivity. *Journal of Clinical Investigation* 2013 **123** 215–223. (https://doi.org/10.1172/JCI62308)

7 Bartelt A, Bruns OT, Reimer R, Hohenberg H, Ittrich H, Peldschus K, Kaul MG, Tromsdorf UI, Weller H, Waurisch C *et al.* Brown adipose tissue activity controls triglyceride clearance. *Nature Medicine* 2011 **17** 200–205. (https://doi.org/10.1038/nm.2297)

8 Becher T, Palanisamy S, Kramer DJ, Eljalby M, Marx SJ, Wibmer AG, Butler SD, Jiang CS, Vaughan R, Schöder H *et al.* Brown adipose tissue is associated with cardiometabolic health. *Nature Medicine* 2021 **27** 58–65. (https://doi.org/10.1038/s41591-020-1126-7)

9 Wibmer AG, Becher T, Eljalby M, Crane A, Andrieu PC, Jiang CS, Vaughan R, Schöder H & Cohen P. Brown adipose tissue is associated with healthier body fat distribution and metabolic benefits independent of regional adiposity. *Cell Reports: Medicine* 2021 **2** 100332. (https://doi.org/10.1016/j.xcrm.2021.100332)

10 Sun L, Yan J, Goh HJ, Govindharajulu P, Verma S, Michael N, Sadananthan SA, Henry CJ, Velan SS & Leow MKS. Fibroblast growth factor-21, leptin, and adiponectin responses to acute cold-induced

brown adipose tissue activation. *Journal of Clinical Endocrinology and Metabolism* 2020 **105** e520–e531. (https://doi.org/10.1210/clinem/dgaa005)
11 Mihalopoulos NL, Yap JT, Beardmore B, Holubkov R, Nanjee MN & Hoffman JM. Cold-activated brown adipose tissue is associated with less cardiometabolic dysfunction in young adults with obesity. *Obesity* 2020 **28** 916–923. (https://doi.org/10.1002/oby.22767)
12 Herz CT, Kulterer OC, Prager M, Schmöltzer C, Langer FB, Prager G, Marculescu R, Kautzky-Willer A, Hacker M, Haug AR *et al.* Active brown adipose tissue is associated with a healthier metabolic phenotype in obesity. *Diabetes* 2022 **71** 93–103. (https://doi.org/10.2337/db21-0475)
13 Franssens BT, Hoogduin H, Leiner T, van der Graaf Y & Visseren FLJ. Relation between brown adipose tissue and measures of obesity and metabolic dysfunction in patients with cardiovascular disease. *Journal of Magnetic Resonance Imaging* 2017 **46** 497–504. (https://doi.org/10.1002/jmri.25594)
14 Chen KY, Cypess AM, Laughlin MR, Haft CR, Hu HH, Bredella MA, Enerbäck S, Kinahan PE, Lichtenbelt WM, Lin FI *et al.* Brown adipose reporting criteria in imaging studies (BARCIST 1.0): recommendations for standardized FDG-PET/CT experiments in humans. *Cell Metabolism* 2016 **24** 210–222. (https://doi.org/10.1016/j.cmet.2016.07.014)
15 Din MU, Raiko J, Saari T, Saunavaara V, Kudomi N, Solin O, Parkkola R, Nuutila P & Virtanen KA. Human brown fat radiodensity indicates underlying tissue composition and systemic metabolic health. *Journal of Clinical Endocrinology and Metabolism* 2017 **102** 2258–2267. (https://doi.org/10.1210/jc.2016-2698)
16 Sanchez-Delgado G, Martinez-Tellez B, Olza J, Aguilera CM, Labayen I, Ortega FB, Chillon P, Fernandez-Reguera C, Alcantara JMA, Martinez-Avila WD *et al.* Activating brown adipose tissue through exercise (ACTIBATE) in young adults: rationale, design and methodology. *Contemporary Clinical Trials* 2015 **45** 416–425. (https://doi.org/10.1016/j.cct.2015.11.004)
17 Acosta FM, Sanchez-Delgado G, Martinez-Tellez B, Migueles JH, Amaro-Gahete FJ, Rensen PCN, Llamas-Elvira JM, Blondin DP & Ruiz JR. Sleep duration and quality are not associated with brown adipose tissue volume or activity-as determined by 18F-FDG uptake, in young, sedentary adults. *Sleep* 2019 **42** zsz177. (https://doi.org/10.1093/sleep/zsz177)
18 Acosta FM, Sanchez-Delgado G, Martinez-Tellez B, Alcantara JMA, Llamas-Elvira JM & Ruiz JR. Diurnal variations of cold-induced thermogenesis in young, healthy adults: a randomized crossover trial. *Clinical Nutrition* 2021 **40** 5311–5321. (https://doi.org/10.1016/j.clnu.2021.08.010)
19 Friedewald WT, Levy RI & Fredrickson DS. Estimation of the concentration of low-density lipoprotein cholesterol in plasma, without use of preparative ultracentrifuge. *Journal of Chemical Information and Modeling* 1972 **53** 1689–1699. (https://doi.org/10.1093/clinchem/18.6.499)
20 Matthews DR, Hosker JP, Rudenski AS, Naylor BA, Treacher DF & Turner RC. Homeostasis model assessment: insulin resistance and β-cell function from fasting plasma glucose and insulin concentrations in man. *Diabetologia* 1985 **28** 412–419. (https://doi.org/10.1007/BF00280883)
21 Wallace TM, Levy JC & Matthews DR. Use and abuse of HOMA modeling. *Diabetes Care* 2004 **27** 1487–1495. (https://doi.org/10.2337/diacare.27.6.1487)
22 Alberti KGMM, Eckel RH, Grundy SM, Zimmet PZ, Cleeman JI, Donato KA, Fruchart JC, James WPT, Loria CM, Smith SC *et al.* Harmonizing the metabolic syndrome: a joint interim statement of the International Diabetes Federation Task Force on Epidemiology and Prevention; National Heart, Lung, and Blood Institute; American Heart Association; World Heart Federation; International Atherosclerosis Society; and International Association for the Study of Obesity. *Circulation* 2009 **120** 1640–1645. (https://doi.org/10.1161/CIRCULATIONAHA.109.192644)
23 Bedogni G, Bellentani S, Miglioli L, Masutti F, Passalacqua M, Castiglione A & Tiribelli C. The fatty liver index: a simple and accurate predictor of hepatic steatosis in the general population. *BMC Gastroenterology* 2006 **6** 33. (https://doi.org/10.1186/1471-230X-6-33)
24 Acosta FM, Martinez-Tellez B, Sanchez-Delgado G, Migueles JH, Contreras-Gomez MA, Martinez-Avila WD, Merchan-Ramirez E, Alcantara JMA, Amaro-Gahete FJ, Llamas-Elvira JM *et al.* Association of objectively measured physical activity with brown adipose tissue volume and activity in young adults. *Journal of Clinical Endocrinology and Metabolism* 2019 **104** 223–233. (https://doi.org/10.1210/jc.2018-01312)
25 Sanchez-Delgado G, Acosta FM, Martinez-Tellez B, Finlayson G, Gibbons C, Labayen I, Llamas-Elvira JM, Gil A, Blundell JE & Ruiz JR. Brown adipose tissue volume and 18F-fluorodeoxyglucose uptake are not associated with energy intake in young human adults. *American Journal of Clinical Nutrition* 2020 **111** 329–339. (https://doi.org/10.1093/ajcn/nqz300)
26 Jurado-Fasoli L, Merchan-Ramirez E, Martinez-Tellez B, Acosta FM, Sanchez-Delgado G, Amaro-Gahete FJ, Muñoz Hernandez V, Martinez-Avila WD, Ortiz-Alvarez L, Xu H *et al.* Association between dietary factors and brown adipose tissue volume/18F-FDG uptake in young adults. *Clinical Nutrition* 2021 **40** 1997–2008. (https://doi.org/10.1016/j.clnu.2020.09.020)
27 Sanchez-Delgado G, Martinez-Tellez B, Acosta FM, Virtue S, Vidal-Puig A, Gil A, Llamas-Elvira JM & Ruiz JR. Brown adipose tissue volume and fat content are positively associated with whole-body adiposity in young men, not in women. *Diabetes* 2021 **70** 1473–1485. (https://doi.org/10.2337/db21-0011)
28 Acosta FM, Martinez-Tellez B, Blondin DP, Haman F, Rensen PCN, Llamas-Elvira JM, Martinez-Nicolas A & Ruiz JR. Relationship between the daily rhythm of distal skin temperature and brown adipose tissue 18F-FDG uptake in young sedentary adults. *Journal of Biological Rhythms* 2019 **34** 533–550. (https://doi.org/10.1177/0748730419865400)
29 Ahmed BA, Ong FJ, Barra NG, Blondin DP, Gunn E, Oreskovich SM, Szamosi JC, Syed SA, Hutchings EK, Konyer NB *et al.* Lower brown adipose tissue activity is associated with non-alcoholic fatty liver disease but not changes in the gut microbiota. *Cell Reports: Medicine* 2021 **2** 100397. (https://doi.org/10.1016/j.xcrm.2021.100397)
30 Karpe F & Pinnick KE. Biology of upper-body and lower-body adipose tissue – link to whole-body phenotypes [Internet]. *Nature Reviews: Endocrinology* 2015 **11** 90–100. (https://doi.org/10.1038/nrendo.2014.185)
31 Rothwell NJ & Stock MJ. A role for brown adipose tissue in diet-induced thermogenesis. *Obesity Research* 1997 **5** 650–656. (https://doi.org/10.1002/j.1550-8528.1997.tb00591.x)
32 Blondin DP, Labbé SM, Noll C, Kunach M, Phoenix S, Guérin B, Turcotte ÉE, Haman F, Richard D & Carpentier AC. Selective impairment of glucose but not fatty acid or oxidative metabolism in brown adipose tissue of subjects with type 2 diabetes. *Diabetes* 2015 **64** 2388–2397. (https://doi.org/10.2337/db14-1651)
33 Muzik O, Mangner TJ, Leonard WR, Kumar A, Janisse J & Granneman JG. 15O PET measurement of blood flow and oxygen consumption in cold-activated human brown fat. *Journal of Nuclear Medicine* 2013 **54** 523–531. (https://doi.org/10.2967/jnumed.112.111336)
34 Bartelt A, John C, Schaltenberg N, Berbée JFP, Worthmann A, Cherradi ML, Schlein C, Piepenburg J, Boon MR, Rinninger F *et al.* Thermogenic adipocytes promote HDL turnover and reverse cholesterol transport. *Nature Communications* 2017 **8** 15010. (https://doi.org/10.1038/ncomms15010)
35 Wang GX, Zhao XY, Meng ZX, Kern M, Dietrich A, Chen Z, Cozacov Z, Zhou D, Okunade AL, Su X *et al.* The brown fat-enriched secreted factor Nrg4 preserves metabolic homeostasis through attenuation of hepatic lipogenesis. *Nature Medicine* 2014 **20** 1436–1443. (https://doi.org/10.1038/nm.3713)

36 Virtue S & Vidal-Puig A. Adipose tissue expandability, lipotoxicity and the metabolic syndrome – an allostatic perspective. *Biochimica et Biophysica Acta* 2010 **1801** 338–349. (https://doi.org/10.1016/j.bbalip.2009.12.006)
37 Saari TJ, Raiko J, U-Din M, Niemi T, Taittonen M, Laine J, Savisto N, Haaparanta-Solin M, Nuutila P, Virtanen KA. Basal and cold-induced fatty acid uptake of human brown adipose tissue is impaired in obesity. *Scientific Reports* 2020 **10** 14373. (https://doi.org/10.1038/s41598-020-71197-2)
38 Acosta FM, Martinez-Tellez B, Sanchez-Delgado G, Alcantara JMA, Acosta-Manzano P, Morales-Artacho AJ & Ruiz JR. Physiological responses to acute cold exposure in young lean men. *PLoS ONE* 2018 **13** e0196543. (https://doi.org/10.1371/journal.pone.0196543)
39 Schilperoort M, Hoeke G, Kooijman S & Rensen PCN. Relevance of lipid metabolism for brown fat visualization and quantification [Internet]. *Current Opinion in Lipidology* 2016 **27** 242–248. (https://doi.org/10.1097/MOL.0000000000000296)

Received 10 February 2022
Revised version received 2 April 2022
Accepted 11 May 2022